

# A Real-Time Software Defined Radio Platform for LTE-Advanced Heterogeneous Networks

Peng Li<sup>1,2</sup>, Yunjian Jia<sup>1</sup>, Mingjun Feng<sup>1</sup>, Changrong Ye<sup>1</sup>, Fei Chen<sup>1</sup>, and Huifang Fan<sup>1</sup>

<sup>1</sup>College of Communication Engineering, Chongqing University, Chongqing, 400044, China

<sup>2</sup>School of Electronic and Electrical Engineering, Chongqing University of Arts and Sciences, Chongqing, 402160, China

Email: {lipeng663073, yunjian, fengmingjun, yechangrong, chenfei, fanhuifang}@cqu.edu.cn

**Abstract**—This paper presents the design and implementation of a LTE-Advanced system platform based on software defined radio. The platform has flexible implementation; common construction; strong ability of modular, expansibility and portability; easy to improve and extend; suitable for testing and verifying evolving LTE-Advanced system. With the platform, we conduct real-time experiments for investigating LTE-Advanced Heterogeneous Networks and the interference management schemes in real wireless environments. The results of real-time experiments truly reflected the influence of channel environment and interference to heterogeneous networks. In the situation without interference management, the Bit Error Rate of user equipments in heterogeneous networks is as high as 30-40% due to the interference. Therefore, user equipments cannot communicate properly. When the interference management scheme is used, user BER drops significantly. At the same time, the throughput of users decreases slightly from that without interference management. The throughput of the users decline slightly and the BER decreases obviously, in return.

**Index Terms**—Software defined radio, platform, LTE-Advanced, heterogeneous networks, interference managements

## I. INTRODUCTION

Fueled by the popularity of smart phones, mobile data traffic has been increasing explosively [1]. To meet rapidly growing demands for high data rate wireless services, a set of radio access technologies have been proposed and developed by the 3rd Generation Partnership Project (3GPP), called Long-Term Evolution (LTE) [2]. Standards development for LTE continues toward establishing an enhancement called LTE-Advanced that can respond to future challenges [3]. In LTE-Advanced, Heterogeneous Networks (HetNet) are one of features as efficient deployments of future mobile networks in which multiple low power low-cost Base Stations (BSs), also called Low Power Nodes (LPNs), are deployed in the presence of an overlaid macro cell [4]. HetNet is envisioned to enhance cellular networks by

offloading traffic from the macro cell, providing higher data rates and dedicated capacity to hot spots.

HetNet as a novel wireless network architecture makes the cellular network more flexible and complicated. Since LPNs, which serve small cells such as femtocell and picocell, have variable capabilities and functions, it is important to investigate HetNet in real wireless environments. Furthermore, one important deployment scenario of HetNet is co-channel deployment, where two different base stations using the same frequency [5], [6]. To cope with the interference between macro cell and small cell, 3GPP has developed an interference management method called enhanced Inter-Cell Interference Coordination (eICIC) for LTE-Advanced [7]. eICIC is a time domain interference coordination scheme to reduce the macro cell to small cell co-channel interference by configuring Almost Blank Subframes (ABS) on macro base stations [8], [9].

However, the interference management scheme is to be updated continuously as well as the LTE-advanced standard itself. Therefore, motivated by the above issues, we develop a reconfigurable and extensible system platform for real-time experiments of LTE-Advanced HetNet based on Software Defined Radio (SDR). SDR originally means to implement physical layer functions by programmable software instead of dedicated hardware in the radio communication system [10], [11]. Now its application has been extended to realize full wireless protocol stack for wireless systems [12], [13].

In this paper, we describe the design and implementation of our SDR platform for LTE-Advanced systems. In the process of constructing platform, the test requirements of LTE-Advanced HetNet are analyzed and summarized; composition structure is designed according to the test requirements; work mode is designed to platform; the functions of each module are fulfilled; Graphical User Interface (GUI) is programmed. We realize operation control, working mode selection and observing the results of the platform depending on GUI.

With the platform, we complete a real-time demonstration of LTE-Advanced HetNet and demonstrate its feasibility and effects in real radio environments. The results show that the platform capable of running. The result of real-time demonstration truly reflected the influence of channel environment and interference to HetNet.

---

Manuscript received September 17, 2015; revised March 4, 2016.

This work is supported by the National High-tech R&D Program of China (863 Program) under grant No.2015AA01A706 and the Scientific and Technological Research Program of Chongqing Municipal Education Commission under grant No.KJ1501107. This work is also sponsored in part by Hitachi, Ltd.

Corresponding author email: yunjian@cqu.edu.cn.

doi:10.12720/jcm.11.3.263-271

The rest of the paper is organized as follows. Section II is the overview of the platform. Section III presents the key issues in building platform. Section IV shows the experiments and results using the platform. Finally, Section V concludes our work.

## II. OVERVIEW OF THE PLATFORM

In this section, we describe the logical architecture emulated by the platform and the actual components and

tools we used.

### A. Logical Architecture Emulated by the Platform

Fig. 1 shows the logical architecture emulated by our platform, which consists of three main parts: centralized BS baseband processor pool, front-haul connecting BS baseband processor pool and BS RF ends, heterogeneous radio access network consisting of RF ends of macro BSs and LPNs.

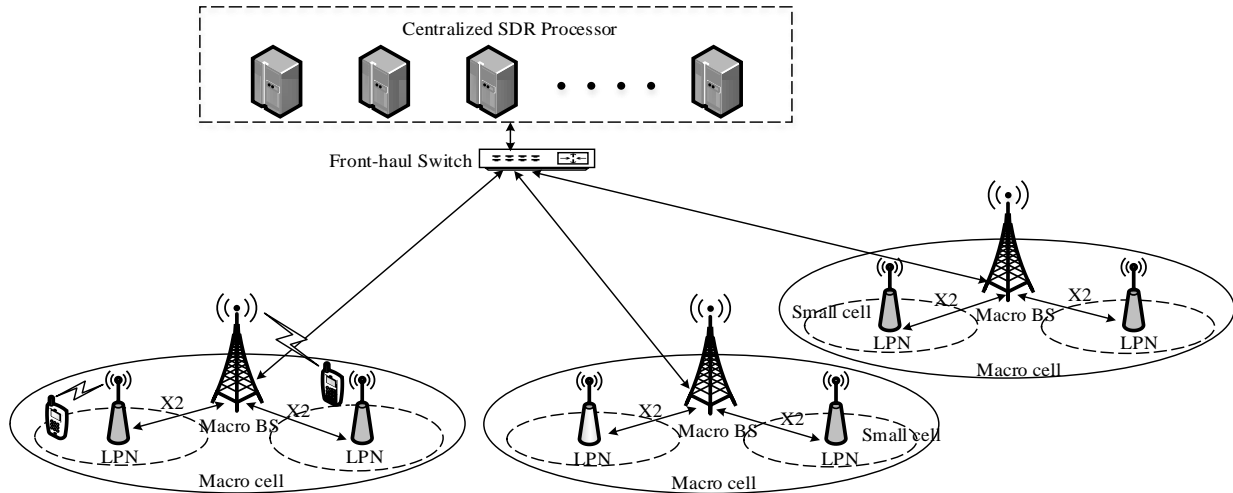


Fig. 1. Logical architecture emulated by the platform

There are two reasons why our platform emulates the cellular systems with the Cloud Radio Access Network (C-RAN) architecture. First, the concept of C-RAN has been regarded as a promising architecture for future cellular networks [14]. Second, we can easily divide the system into the components emulated by SDR, where SDR programmable software can implement the functions of the centralized BS baseband pool, and supplied RF transceiver for SDR signals which can work as the BS RF ends.

### B. Actual Components Used in the Platform

We choose the following SDR development platform and devices to realize the platform which has the above logical architecture.

We use GNU Radio to create SDR digital signals. GNU Radio is an open-source software development toolkit that provides signal processing blocks to implement wireless protocols [15]. Since GNU Radio is able to implement real-time, high throughput radio systems in a simple-to-use, rapid application development environment, it is widely used in academia and industry to support both wireless communications research and real radio systems. Furthermore, since it can provide a friendly interactive interface, we also use it to make the experiment results visual.

Since GNU Radio can only handle digital data, we use USRP from Ettus Research [16] as the RF front end to shift baseband signals to the desired center frequency. USRP series include different motherboards with interfaces such as USB and Gigabit Ethernet, with the

sampling rates up to 100 Msps and a range of frontends for reception and transmission up to 5.8 GHz. In our platform, we use USRP N210 where the on-board oscillator runs at the frequency 100 MHz, with the frequency stability of 2.5 ppm. One SBX daughterboard with one antenna which can operate in the 2.4 GHz band is equipped at each USRP N210.

We choose a Dell Power Edge T620 Server as the SDR processor, where we run GNU Radio to realize the baseband signal processing and transformation. Its high-performance computing capabilities meets the need for information processing of the platform.

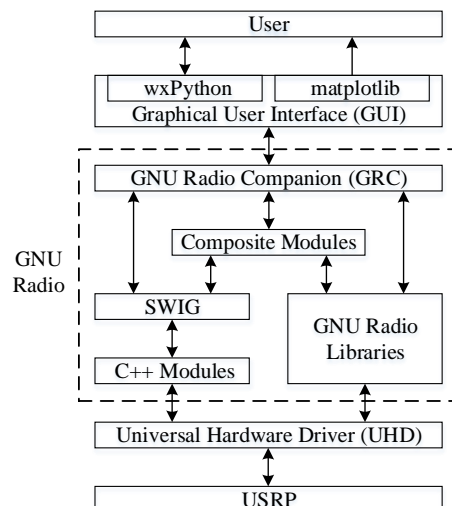


Fig. 2. Schematic diagram of SDR implementation in the platform

We choose TP-LINK TL-SG1024DT to connect USRPs with the SDR processor to achieve rapid signal transmission. The transmission rate is up to 1000Mbps, which fully meets the needs of our platform.

Fig. 2 shows the corresponding SDR implementation in the GNU Radio we programmed. Users send command to GNU Radio through GUI to control signal processing flow. Universal Hardware Driver (UHD) is the bridge of GNU Radio and USRP. GNU Radio can operate and

control USRP through UHD. Signal processing flow is the core of SDR implementation. Signal processing flow is made up of several signal processing modules which is organized and connected by Python. Signal processing modules can be programmed by both Python and C++, except performance-critical modules which must be programmed by C++. Through SWIG, signal processing flow calls signal processing modules programmed by C++.

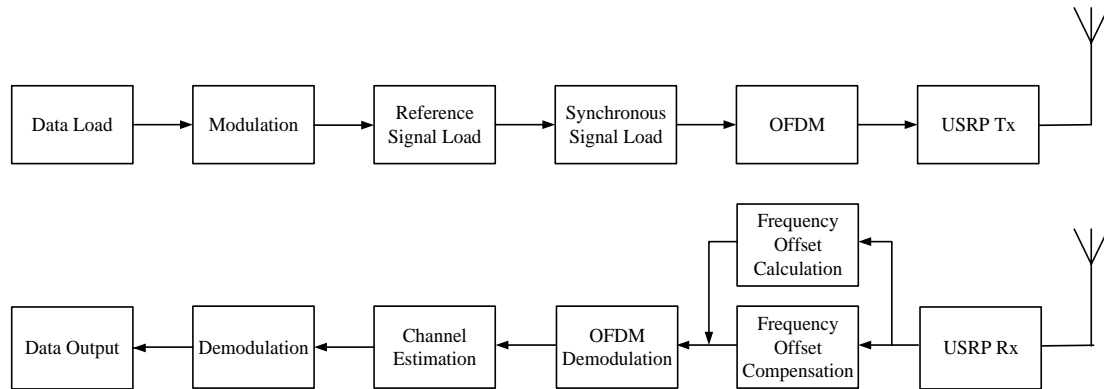


Fig. 3. The procedure of signal processing at the transmitter and the receiver

C. General LTE-Advanced Protocol Implementation

The physical layer processing in the SDR platform conforms to 3GPP LTE-Advanced technical specifications [17]. The main baseband signal processing flows of the transmitter and receiver are illustrated in Fig. 3. According to the LTE-Advanced physical layer protocol, we implement an Orthogonal Frequency Division Multiplexing (OFDM) signal transceiver in the platform, where the control signaling structures are totally assigned to the corresponding time-frequency domain resource block. Using the control signaling, User Equipment (UE) can obtain synchronization and distinguish signals from different BSs. As an implementation issue, channel estimation at UE uses a conventional 2D MMSE scheme.

D. Interference Management for LTE-Advanced HetNet

The LTE-Advanced HetNet has been equipped with not only macro base station but also a lot of LPNs, including picocell base station (Pico), femtocell base station (Femto), relay station (Relay) and radio remote unit (RRH) [18]. The access nodes classifications in the HetNet are made according to the base station transmit power, coverage size and the types of backhaul as shown in Table I.

TABLE I: THE ACCESS NODES CLASSIFICATIONS OF HETNET

Types of nodes	Transmit power	Coverage	Backhaul
Macro BS	46 dBm	Few km	S1 interface
Pico	23-30 dBm	< 300 m	X2 interface
Femto	< 23 dBm	< 50 m	Internet IP
Relay	30 dBm	300 m	Wireless
RRH	46 dBm	Few km	Fiber

A large number of LPNs are introduced in the HetNet. It could reduce the distance between the wireless

communication network and users; increase network capacity; shunt the load of macro cell; improve spectrum efficiency; enhance indoor coverage; develop the cell edge users' communication quality and reduce the costs of operation and maintenance [19]. On the other hand, intensive deployment of LPNs in HetNet will form numerous small cells in macro cells, which produce large amounts of cell edges. The large amounts of cell edges will result in various interferences in different types. Therefore, we must suppress inter-cell interference in order to guarantee that the user in HetNet can communicate normally.

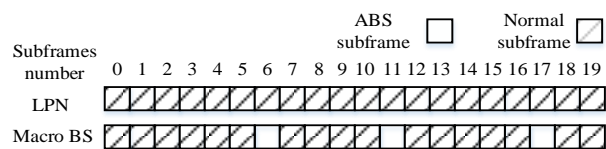


Fig. 4. An example of ABS patterns for eICIC

Inter-cell interference management is one of the most important issues in HetNet. The eICIC, as an interference management solution for LTE-Advanced HetNet, has been studied for the initial feasibility tests and computer simulations in 3GPP [20]. We implement the eICIC scheme called ABS in our platform for the real-world experiments of HetNet. ABS can be used to mitigate downlink data interference from macro BS to the UEs of the LPN. ABS patterns are configured at macro BS. Fig. 4 shows an example of ABS patterns with the TABS of 20m, by which macro BS may transmit almost blank subframes, i.e., zero or less power data transmission, in the subframes numbered 6, 11, and 17. The information on ABS patterns can be sent from macro BS to LPN via the X2 interface. Then the LPN can decide its scheduling, taking into account the ABS patterns, i.e., schedule the

UE located at the small cell edge to the resource blocks when the macro BS transmits the ABS.

### III. KEY ISSUES IN BUILDING PLATFORM

There are two key issues during the building of the platform. One is wireless transceiver working mode selection and implementation; the other is the transmitter and receiver synchronizing and tracking.

#### A. Transmitter and Receiver Program Based on Event-Driven

The transmitter and receiver adopt event-driven working mode in the platform. Both transmitter and receiver have several different states. State transition is triggered by external events.

As shown in Fig. 5, the transmitter has three states which are unstarted state, wait state, and transmit state.

The transmitter generates baseband data conforms to the LTE-Advanced specification. The platform accepts users' commands through the GUI. The transmitter shifts from unstarted state to wait state by calling GUI control `top_block.start()`. When the GNU Radio cache has data to transmit, the transmitter state shifts from wait state to transmit state; when there is no data to send, the transmitter state stays in wait state. In wait state, the transmitter still sends control information. Under transmit state, if the cache of the GNU Radio still has data to transmit, the transmitter will continue to send data and control information, until the data has been sent completely or the GUI control `top_block.wait()` has been triggered by external events. When transmitter GUI control `top_block.stop()` is valid, the transmitter stops transmitting data and returns to unstarted state.

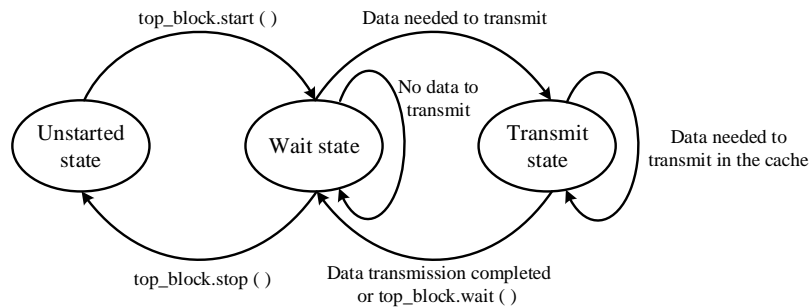


Fig. 5. The state transition diagram of the transmitter

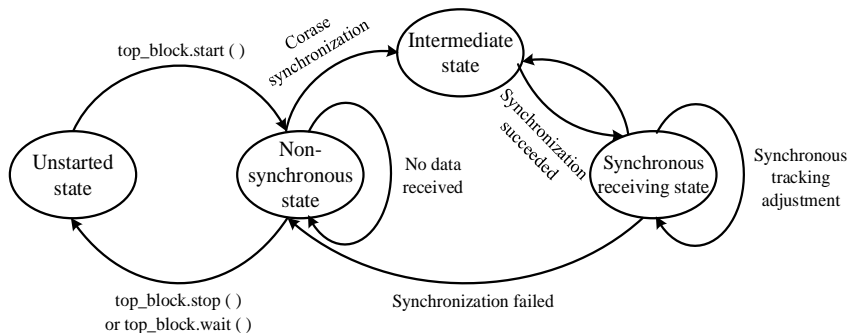


Fig. 6. The state transition diagram of the receiver

It can be seen from Fig. 6 that the receiver has four states which are unstarted state, non-synchronous state, intermediate state and synchronous receiving state. The receiver shifts from unstarted state to non-synchronous state by calling GUI control `top_block.start()`. In non-synchronous state, the receiver doesn't decode, but does coarse synchronization work through the signal received. If no datum is received, then the receiver makes synchronization frequently after intervals. If there are some data to receive, then it does coarse synchronization work by using Primary Synchronization Signal (PSS). The state of receiver shifts from non-synchronous state to intermediate state.

The function of the intermediate state is to realize the frame alignment of the GNU Radio cache. Both transmitter and receiver of the platform have PSS and Secondary Synchronization Signal (SSS) in wireless

frame. The PSS and SSS are used to realize synchronization and get the ID of the base station. The receiver makes sliding correlation through PSS in received signal and PSS generated in local. It can determine the location of the PSS in the received signal according to the location of the correlation peak. As shown in Fig. 7, the PSS in slot 0 and the PSS in slot 10 are the same, while the SSS in slot 0 and SSS in slot 10 are different. So we can realize half frame synchronization by PSS. At this time, the starting position of the frame can be determined according to the location of SSS because the distance between PSS and SSS is fixed. After achieving the starting position of the frame, we can utilize the discarding function of the GNU Radio to discard the unaligned data. The cache data of the GNU Radio then becomes aligned in the next cycle. Finally, the cache has a complete frame of baseband data.

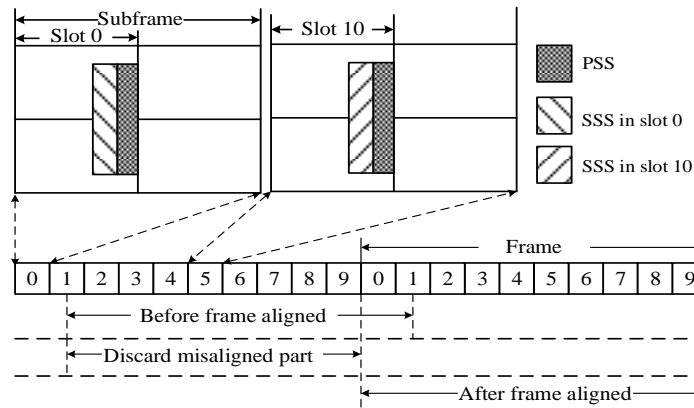


Fig. 7. The frame alignment of GNU Radio cache data

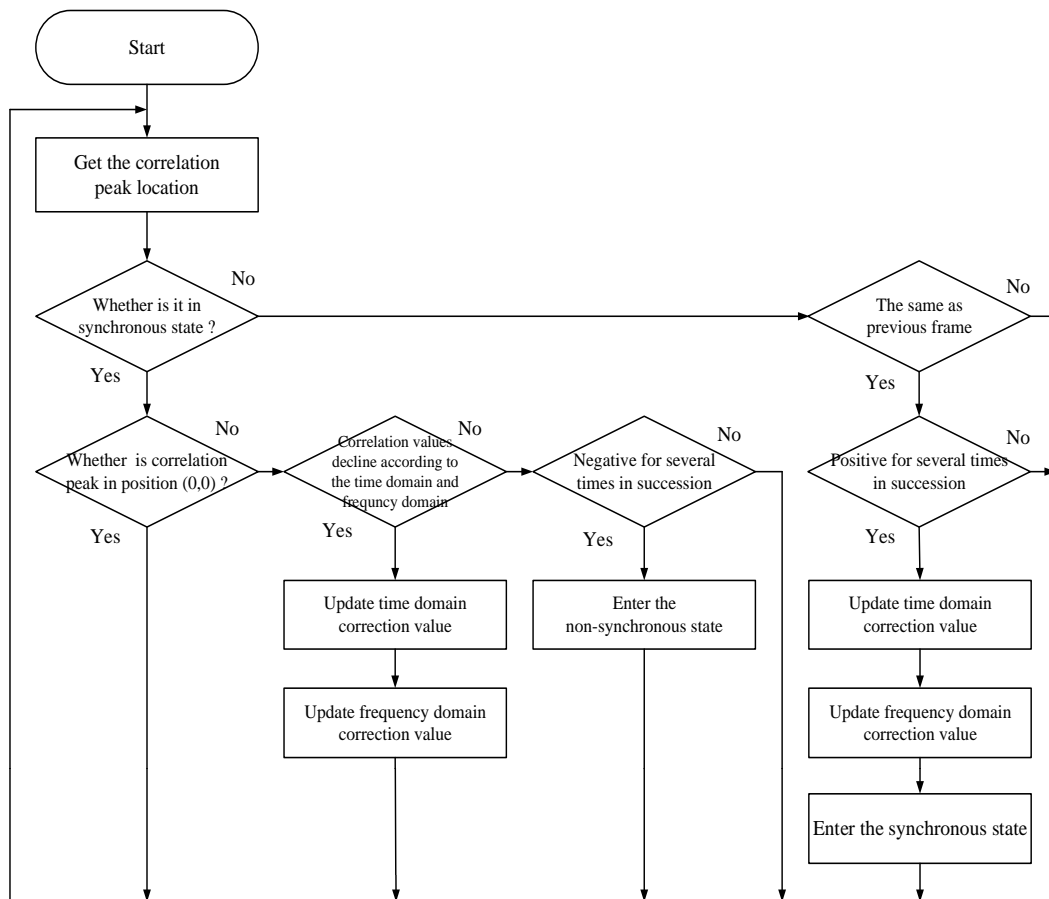


Fig. 8. The flow chart of synchronizing and tracking

The receiver enters into synchronous receiving state, after the receiver and the transmitter have been synchronized successfully. In this state, the receiver keeps on synchronous tracking adjusting in order to ensure the receiver stay in synchronous state when time domain and frequency domain offset slightly. The receiver won't return to non-synchronous state until synchronization failed.

### B. Synchronizing and Tracking

The process of synchronous tracking and synchronous deciding is shown in Fig. 8. The receiver can get the location of the correlation peak after it is started. If the

receiver is in synchronous state in previous cycle then it can decide whether correlation peak is in central position (0, 0). The receiver is in synchronous state if the correlation peak is in central position (0, 0) and no adjustment is needed here. On the contrary, if it is not in central position (0, 0), the receiver decides whether correlation values declines according to time domain and frequency domain. It indicates that the receiver offsets slightly if correlation values declines accordingly. Then the synchronous point should be adjusted to the location of correlation peak. If not, the receiver is in non-synchronous state then the synchronous procedure should be performed to make the receiver enter into synchronous

state again. In synchronous procedure, the received data are compared with previous data. If the data are the same, it suggests a loss in synchronization of the communication link; the receiver is in non-synchronous state. A lot of consecutive decisions in the flow chart can avoid frequent switches of receiver state caused by burst interference. Then the synchronous point is calculated by PSS and SSS. The receiver reenters into synchronous state by updating time domain correction value and frequency domain correction value.

IV. EXPERIMENTS AND RESULTS

After platform has been built, we carry out real-time communication in real radio environment. Then we select Ettus Research USRP N210 as the base station RF front end and wireless terminal. The Dell Power Edge T620 server is the Central Processing Unit (CPU). The GNU Radio is installed in the CPU to realize baseband digital signal processing. The macro BS is connected with the CPU by a wired backhaul way through the front-haul switch. Similarly, LPNs are connected with the macro BS by wired backhaul. The parameter configuration of platform is shown in Table II.

TABLE II: PARAMETER CONFIGURATION OF THE PLATFORM

Parameter	Value
Macro BS Tx power	46 dBm
LPN Tx power	23 dBm
System bandwidth	5 MHz
Carrier frequency	2.4 GHz
Sampling Rate	7.68 MHz
Number of Tx antennas	2
Number of Rx antennas	2
Antennas gain	3 dBi
Backhaul	Wired

We use the platform to perform real-time communication of three HetNet scenarios in real radio environments. They are shown in Fig. 9, Fig. 10 and Fig. 11 respectively. In Scenario 1, only macro BS is working

while the LPNs are switched off in the network. All users are served by the macro BS. This scenario represents the conventional homogeneous cellular networks. In Scenario 2, both macro BS and LPN are working. UE 1 is served by the LPN and UE 2 is served by the macro BS, while no interference management is used for this scenario. It means that either of the UEs is suffering severe inter-cell interference. This scenario presents the situation of HetNet deployment without eICIC. Scenario 3 is similar to Scenario 2 except for the interference management, where eICIC is used to handle the inter-cell interference.

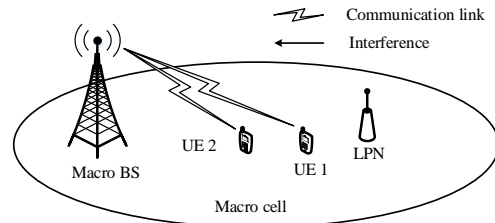


Fig. 9. Scenario 1, Macro BS works only

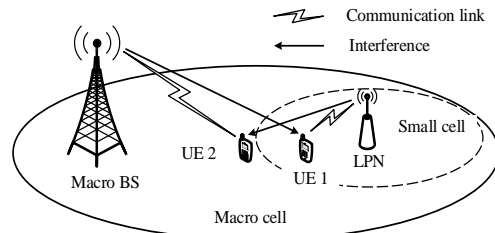


Fig. 10. Scenario 2, two-tier macro cell-small cell HetNet without eICIC

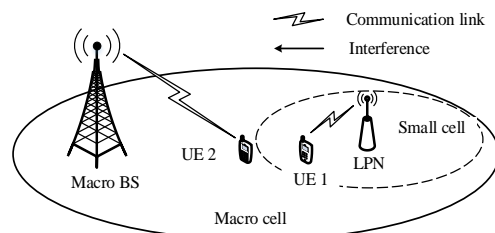


Fig. 11. Scenario 3, two-tier macro cell-small cell HetNet with eICIC

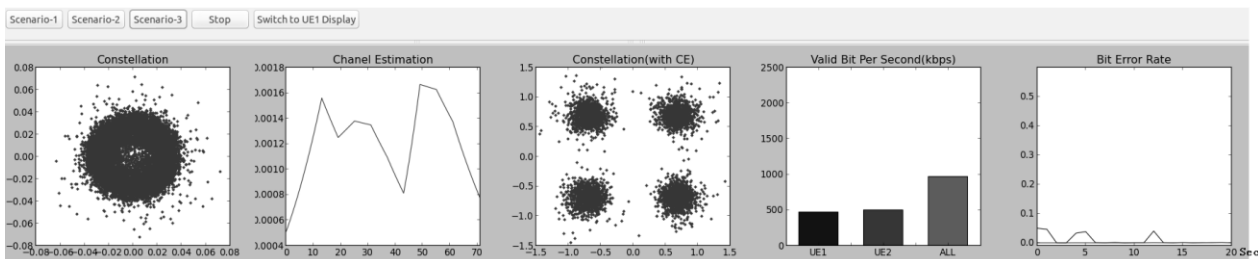


Fig. 12. A snapshot of the real-time experiment results from GUI

We also develop a GUI to monitor the real-time system performance in the experiments. The GUI of platform is programmed by WxPython as shown in Fig. 12. This figure is a snapshot of the real-time experiment results from GUI display when the platform is working in Scenario 3. The received baseband signals, the demodulated signals before turbo decoding, the throughput, and the Bit Error Rate (BER) at each UE are shown from left to right, respectively. We use color blue

to represent UE 1 and color red to represent UE 2. In addition, the green column in the throughput figure is the sum of the throughputs of UE 1 and UE 2 in order to represent the total system throughput. The experiment results demonstrate that both small cell UE 1 and macro cell UE 2 can receive the signals normally.

The throughput and BER of the users are two important performance indexes. Fig. 13 shows the BER of users in HetNet without and with eICIC. In this figure,

the horizontal axis is about the change of time and the vertical axis shows that of BERs. Fig. 14 shows the throughput of users in HetNet without and with eICIC. The horizontal axis reveals the change of time and the vertical axis shows that of user throughputs.

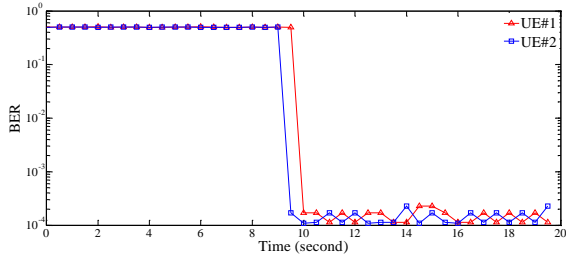


Fig. 13. The contrast of BERs without and with eICIC

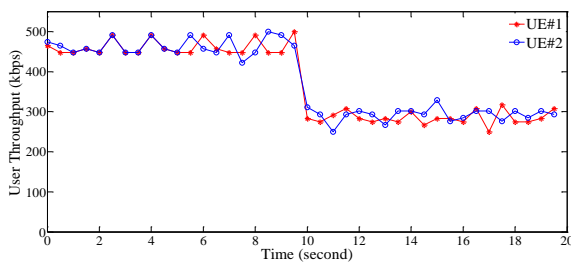


Fig. 14. The contrast of user throughputs without and with eICIC

In the situation without eICIC, the communication rates of both small cell UE 1 and macro cell UE 2 are about 450 Kbps. However, the BER of UEs is as high as 30-40% due to the inter-cell interference. Therefore, UEs cannot communicate properly. When the eICIC is used at about the 10th second, user BER drops significantly. At the same time, the throughput of users decreases slightly from that without eICIC to about 300 kbps because there are some subframes carrying no data. The slight decline of throughput of the users causes the obvious decrease of BER. The throughput of the users decline slightly and the BER decreases obviously, in return.

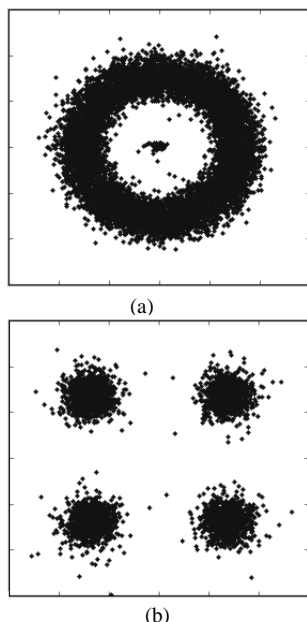


Fig. 15. The constellations before and after the phase correction.

Fig. 15 shows the constellations before and after the phase correction. Platform uses QPSK modulation. After synchronization and Fast Fourier Transformation (FFT), the receiver obtains a frame data. The positioning error of the FFT window leads to the rotation of constellation point. While the Inter-Carrier Interference (ICI) leads to cloud divergence of constellation. As a result, the band-shaped ring is formed as in Fig. 15 (a). After the phase correction is adopted, constellation points of the received data are gathered again in positions of  $\pi/4$ ,  $3\pi/4$ ,  $5\pi/4$ , and  $7\pi/4$  of the signal space.

## V. CONCLUSIONS

This paper focuses on LTE-Advanced systems and presents the design and implementation of a platform based on SDR. We use GNU Radio and USRP to achieve a reconfigurable and low cost platform capable of emulating LTE-Advanced HetNet. The real-time experiments demonstrate the effects of a LTE-Advanced HetNet interference management scheme. This work can serve as the basis to bring HetNet study into the system implementation field.

Future work will take into consideration the multiple antennas deployed at both transmitters and receivers. Message Passing will be adopted to transmit control information between the modules of the platform. By doing this, the computational resource consumption of the platform control information transmission is reduced. The platform will adopt extended instruction set supported by its processor in order to improve the processing speed. Furthermore, expanding the scale of the system platform with more advanced wireless technologies and network structures will be investigated in real radio environments.

## ACKNOWLEDGEMENT

We would like to thank the anonymous referees whose comments helped us to improve the presentation of this paper. This work is supported by the National High-tech R&D Program of China (863 Program) under grant No.2015AA01A706 and the Scientific and Technological Research Program of Chongqing Municipal Education Commission under grant No. KJ1501107. This work is also sponsored in part by Hitachi, Ltd.

## REFERENCES

- [1] Cisco, "Cisco visual networking index: Global mobile data traffic forecast update, 2013-2018," White Paper, Cisco, Feb. 2014.
- [2] E. Dahlman, S. Parkvall, and J. Skööld, *4G-LTE/LTE-Advanced for Mobile Broadband*, New York: Academic Press, 2011.
- [3] A. Ghosh, R. Rattasuk, B. Mondal, N. Mangalvedhe, and T. Thomas, "LTE-Advanced: Next-Generation wireless broadband technology," *IEEE Wireless Commun.*, vol. 17, no. 3, pp. 10-22, June 2010.

- [4] A. Damnjanovic, J. Montojo, Y. Wei, T. F. Ji, T. Luo, M. Vajapeyam, *et al.*, "A survey on 3GPP heterogeneous networks," *IEEE Wireless Commun.*, vol. 18, no. 3, pp. 10-21, June 2011.
- [5] D. Lopez-Perez and X. Chu, "Inter-cell interference coordination for expanded region picocells in heterogeneous networks," in *Proc. 20th International Conference on Computer Communications and Networks*, Hawaii, USA, 2011, pp. 1-6.
- [6] D. Lopez-Perez, İ. Güvenc, G. D. L. Roche, M. Kountouris, T. Q. S. Quek, and J. Zhang, "Enhanced intercell interference coordination challenges in heterogeneous networks," *IEEE Wireless Commun.* vol. 18, no. 3, pp. 22-30, June 2011.
- [7] 3GPP Technical Document R1-104968. Summary of the Description of Candidate eICIC Solutions, in Contribution at 3GPP Meeting in Madrid, Spain, August 2010.
- [8] U. Serkan, T. Hidekazu, and B. Zubin, "Protection of cell-edge users in wireless systems by using almost blank subframes," in *Proc. 9th International ITG Conference on Systems, Communication and Coding*, München, Germany, 2013, pp. 1-6.
- [9] S. N. S. Kshatriya, S. Kaimalettu, S. R. Yerrapareddy, K. Milleth, and N. Akhtar, "On interference management based on subframe blanking in heterogeneous LTE networks," in *Proc. 5th International Conference on Communication Systems and Networks*, Bangalore, 2013, pp. 1-7.
- [10] H. V. Balan, M. Segura, S. Deora, A. Michaloliakos, R. Rogalin, K. Psounis, *et al.*, "USC SDR, an easy-to-program, high data rate, real time software radio platform," in *Proc. 2nd ACM SIGCOMM Workshop on Software Radio Implementation Forum*, Hong Kong, 2013, pp. 25-29.
- [11] Z. Zhao, G. Yang, Q. Liu, K. Li, and L. Cui, "Implementation and application of a multi-radio wireless sensor networks testbed," in *Proc. 4th IET Wireless Sensor Systems*, 2011, pp. 191-199.
- [12] H. Wang, W. Jouini, A. Nafkha, J. Palicot, L. S. Cardoso, M. Debbah, *et al.*, "Blind standard identification with bandwidth shape and GI recognition using USRP platform and SDR4all tools," in *Proc. 5th International Conference on Cognitive Radio Oriented Wireless Networks & Communications*, Cannes, 2010, pp. 1-5.
- [13] Z. Huang, W. Wang, and Y. Zhang, "Design and implementation of cognitive radio hardware platform based on USRP," in *Proc. IET International Conference on Communication Technology and Application*, Beijing, 2011, pp. 160-164.
- [14] China Mobile Research Institute, C-RAN the Road Towards Green RAN, White Paper, China Mobile Research Institute, October 2011.
- [15] GNU Radio Website. [Online]. Available: <http://www.gnuradio.org>
- [16] Ettus Research Website. [Online]. Available: <http://www.ettus.com>
- [17] TS 36.211, Evolved Universal Terrestrial Radio Access (E-UTRA); Physical Channels and Modulation, 3GPP, 2011.
- [18] A. Ghosh, N. Mangalvedhe, R. Ratasuk, B. Mondal, M. Cudak, E. Visotsky, *et al.*, "Heterogeneous cellular networks: from theory to practice," *IEEE Communications Magazine*, vol. 50, no. 6, pp. 54-64, June 2012.
- [19] 3GPP, Technical Document R1-130754: System Simulation Results on Heterogeneous Networks with cell Range Extension, Renesas Mobile Europe Ltd.
- [20] 3GPP, Evolved Universal Terrestrial Radio Access (E-UTRA) and Evolved Universal Terrestrial Radio Access Network (E-UTRAN); Overall Description; Stage 2, 3GPP Tech. Spec. TS 36.300, Ver. 10.8.0, July 2012.



**Peng Li** received his Bachelor's degree in Electronic Science and Technology from Si Chuan University, Cheng Du, in 2004. He received his Master's degree in Communication and Information System from Chong Qing University, Chong Qing, in 2010. He has been studying Communication and Information System in College of Communication Engineering, Chongqing University, Chongqing, since 2012. He has actively contributed to design and implementation of LTE, LTE-Advanced physical layer and MAC layer by software defined radio. He is researching SDR, Cognitive Radio and LTE-Advanced HetNet. Since 2010, he has been working as an lecturer in School of Electronic and Electrical Engineering, Chongqing University of Arts and Sciences, Chongqing, China.



**Yun-Jian Jia** received his B.S. degree from Nankai University, China, and his M.E. and Ph.D. degrees in Engineering from Osaka University, Japan, in 1999, 2003 and 2006, respectively. From 2006 to 2012, he was a Researcher with Central Research Laboratory, Hitachi, Ltd., where he engaged in research and development on wireless networks and contributed to LTE/LTE-Advanced standardization in 3GPP. He is now a professor at the School of Communication Engineering, Chongqing University, Chongqing, China. He is the author of more than 40 papers, more than 60 inventions, and more than 30 technical documents of 3GPP. He is a member of IEEE and IEICE, and holds 19 patents. His research interests include multiple-antenna technologies, 4G and beyond wireless communications systems, resource management of mobile networks.

**Ming-Jun Feng** received his Bachelor's degree in Electronic Information Science and Technology from Central South University, China, in 2013. He is currently working toward the Master's degree in Communication and Information System in College of Communication Engineering, Chongqing University,

Chongqing, China. He mainly engages in research of Software Defined Radio and Cognitive Radio.

**Chang-Rong Ye** received his Bachelor's degree in College of Communication and Engineering in Chongqing University, China, in 2011. He is currently working toward the Doctor's degree in Circuits and System in the same college and university. He mainly engages in research and implementation of SDR real-time communication system, just like CW, PSK31 and parts of the physical links of LTE-Advanced. He is researching in algorithm of decoding the telemetry form the amateur radio satellite. He is also research the Frequency Division Multiplex Digital Voice (FDMDV) system implementation.

**Fei Chen** received his Bachelor's degree in electronics engineering from the Communication Institute, China, his Master's degree in Signal and Information Processing from Chongqing University of Posts and Telecommunications, China, and the Doctor's degree in Circuits and System from Chongqing University, China, in 2000, 2009 and 2012 respectively. He is currently an associate professor of Chongqing Communication Institute, China. His research efforts have been associated with statistical signal processing and detection of physiological recordings. he is working on the extraction of fetal cardiac signals. he has also worked in industry on the design and implementation of digital electronics and software in wireless body sensor networks.

the reason is that the time window referring to this point is 0:00-4:00. During such period, a cab is more likely to stay at a fixed location, which decreases the contacts with other cabs. As previously described, *Roma* covers larger urban area than *Cabspotting*, which dilutes the node density and implicitly reduces the contact probability. Therefore, the Median of *Roma*'s *PI* is about 58 percent. *Infocom05* and *Calabria* present superior periodicity since the Medians of *PI* are about 74.3 and 84.3 percent respectively. The most remarkable point is the *PI* of the third time window in *Infocom05*, i.e., 96.67%. This agrees with the fact that people always stay in a fixed conference site everyday based on uniform meeting schedule. To our best knowledge, this is the first approach that quantitatively measures the *periodicity* of realistic mobility traces. Above all, we show that the *periodicity* does exist in *MSNs* and *VANET*.

**B. Path Redundancy**

Another un-conspicuous characteristic of realistic mobility trace is *path redundancy*, which is uncovered by the numerical analysis of four data sets. Next, we propose three quantitative metrics to fully represent the degree of *path redundancy* over a time window  $[t_1, t_2]$  as follows:

$$\alpha(t_1, t_2) = \frac{\sum_{(u,v) \in V_c^{[t_1, t_2]}} |P_{u \rightarrow v}^{[t_1, t_2]}|}{|V_c^{[t_1, t_2]}|} \quad (2)$$

$$\beta(t_1, t_2) = \frac{2|V_c^{[t_1, t_2]}|}{|V|(|V|-1)} \quad (3)$$

$$\gamma(t_1, t_2) = \frac{|V_{c'}^{[t_1, t_2]}|}{|V_c^{[t_1, t_2]}|} \quad (4)$$

The variables appeared in Eq. (2)-(4) are defined in Tab II. Observing from Eq. (2), Eq. (3) and Eq. (4), the above indexes  $\alpha, \beta, \gamma$  represent the average path number of connected node-pairs: accumulating the path number of each connected node-pair  $u \rightarrow v$  during  $[t_1, t_2]$  divided by the number of connected node-pairs; the percent of node-pairs that have at least one path: the number of connected node-pairs divided by the number of all possible node-pairs; the percent of connected node-pairs that have more than one path: the number of node-pairs that have redundant paths divided by the number of connected node-pairs; respectively.

To facilitate our analysis, we generate a special data structure, where the value of  $i$ th row and  $j$ th column denotes the neighbor set of node  $j$  in  $i$ th time-slot. Then, all available paths of a node-pair in a given time window can be searched in a *recursive* approach. For all data sets, we investigate  $\alpha, \beta, \gamma$  under various length of time window, denoted as  $T_i$ . To proceed, we fix the value of  $T_i$  orderly from *5min* to *40min* with *5min* in between and

divide one day into 24 hours, then calculate  $\alpha, \beta, \gamma$  over 24 time windows with length  $T_i$ , which are randomly selected from each and every hour, to take the average. Here the value of  $T_i$  is fixed at some discrete values with 5min in between. The reason why we adopt such simplified handling is to decrease recursive depth, which further reduce computational overhead. Suppose we take a fine-grained step unit, i.e., 1min and vary  $T_i$  from 1min to 60min. If  $T_i$  is taken as 10min, the recursive search for any node-pair has to be conducted in a path tree with 10 hops, which yield tremendous computational complexity. Indeed, the revelation of the rising tendency is enough to uncover the desired characteristic.

TABLE II: ANNOTATIONS IN SECTION III-B

$V_c^{[t_1, t_2]}$	The set of connected node-pairs, $(u, v) \in V_c^{[t_1, t_2]}$ if there exists at least one path connecting $(u, v)$ in $[t_1, t_2]$ .
$P_{u \rightarrow v}^{[t_1, t_2]}$	The path-set including all the paths which exist in $[t_1, t_2]$ from $u$ to $v$ .
$V_{c'}^{[t_1, t_2]}$	The set of connected node-pairs, $(u, v) \in V_{c'}^{[t_1, t_2]}$ if there exists more than one path connecting $(u, v)$ in $[t_1, t_2]$ .

As shown in Fig. 2(a), the average path number of all data sets are sharply increasing as we enlarge the time window, since more opportunistic paths with larger delay for any pair of nodes become available. In addition, we present the value of  $\alpha$  in a log-scale to accommodate display. Observing from Fig. 2(b), the  $\beta$  index which reflects the network connectivity is rising up when  $T_i$  varies from *5min* to *40min* but remains within 0.31, which reveals a fact that a realistic network can hardly reach fully-connected state. Fortunately, the medians of  $\gamma$  shown in Fig. 2(c) are 0.95, 0.76, 0.60, 0.55, respectively. It can be seen that path redundancy does exist between connected node-pairs laying the foundation for topology control.

**IV. TOPOLOGY CONTROL**

The existence of *periodicity* and *path redundancy* has been validated in Section III, which substantially provides the feasibility and operability of topology control. In this section, we first model the evolving topology as a space-time graph, then formulate and solve the set cover problem. Last, a topology-control algorithm is proposed based on optimal covering.

**A. Space-Time Graph**

Traditional static graph cannot represent the evolution of contact process among nodes. In fact, one static graph is a snapshot of nodes and their contacts appear at certain time point. To capture such dynamic evolutions, we use a sequence of network snapshots to build a space-time graph [22].